Automated detection of periventricular veins on 7 T brain MRI

Hugo J. Kuijf[a], Willem H. Bouvy[b], Jaco J.M. Zwanenburg[a,c], Max A. Viergever[a], Geert Jan Biessels[b], and Koen L. Vincken[a]

[a]Image Sciences Institute, University Medical Center Utrecht, Utrecht, the Netherlands;
[b]Department of Neurology, Brain Center Rudolf Magnus, University Medical Center Utrecht, Utrecht, the Netherlands;
[c]Department of Radiology, University Medical Center Utrecht, Utrecht, the Netherlands

ABSTRACT

Cerebral small vessel disease is common in elderly persons and a leading cause of cognitive decline, dementia, and acute stroke. With the introduction of ultra-high field strength 7.0 T MRI, it is possible to visualize small vessels in the brain. In this work, a proof-of-principle study is conducted to assess the feasibility of automatically detecting periventricular veins.

Periventricular veins are organized in a fan-pattern and drain venous blood from the brain towards the caudate vein of Schlesinger, which is situated along the lateral ventricles. Just outside this vein, a region-of-interest (ROI) through which all periventricular veins must cross is defined. Within this ROI, a combination of the vesselness filter, tubular tracking, and hysteresis thresholding is applied to locate periventricular veins.

All detected locations were evaluated by an expert human observer. The results showed a positive predictive value of 88 % and a sensitivity of 95 % for detecting periventricular veins.

The proposed method shows good results in detecting periventricular veins in the brain on 7.0 T MR images. Compared to previous works, that only use a 1D or 2D ROI and limited image processing, our work presents a more comprehensive definition of the ROI, advanced image processing techniques to detect periventricular veins, and a quantitative analysis of the performance. The results of this proof-of-principle study are promising and will be used to assess periventricular veins on 7.0 T brain MRI.

Keywords: quantitative image analysis, segmentation methodologies

1. INTRODUCTION

Cerebral small vessel disease is a term commonly used to refer to pathological processes that affect the small vessels of the brain. Small vessel disease is common in elderly persons and a leading cause of cognitive decline, dementia, and acute stroke.[1,2] However, small vessels in the brain cannot be visualized directly with conventional MRI. Hence, manifestations of small vessel disease in the cerebral parenchyma, such as lacunar infarcts, white matter lesions, intracranial haemorrhages, and microbleeds, are often investigated.[1,2] Unfortunately, these so-called parenchymal lesions only represent a limited subset of the manifestations of small vessel disease and more advanced imaging is needed to capture its full spectrum.

With the introduction of ultra-high field strength 7.0 T MRI, it has become feasible to image small vessels directly.[2–5] This is demonstrated in Figure 1, where small periventricular veins can be seen. These periventricular veins drain venous blood from the brain towards the subependymal veins (such as the caudate vein of Schlesinger), which run in parallel with the lateral ventricles. In a coronal view (Figure 1b), the typical fan-pattern of these veins can be appreciated.[6]

Corresponding author:
Hugo J. Kuijf, Image Sciences Institute, University Medical Center Utrecht, Heidelberglaan 100, Room Q.02.445, 3584 CX, Utrecht, the Netherlands. E-mail: hugok@isi.uu.nl. Phone: +31 88 75 58562.

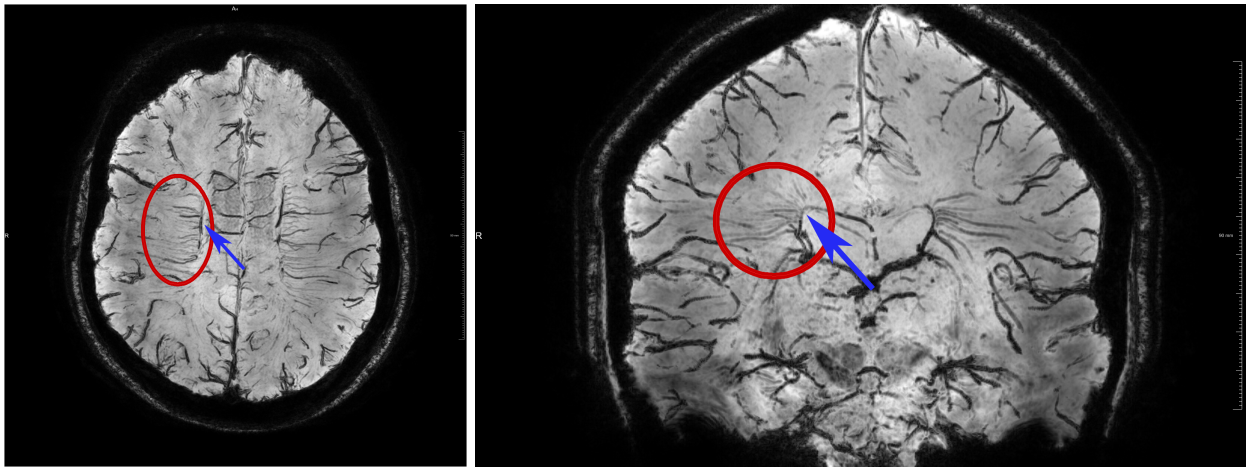

(a) (b)

Figure 1: A transversal (a) and coronal (b) minimum intensity projection (minIP, slab of 30 slices / 10.5 mm) view of a 7.0 T T2*-weighted MRI acquisition, showing periventricular veins. Veins are encircled (in red) in one hemisphere and visible at the same location in the contralateral hemisphere. They originate from the deep white matter of the brain, in a typical "fan-pattern", and drain venous blood towards the caudate vein of Schlesinger (blue arrow).[6]

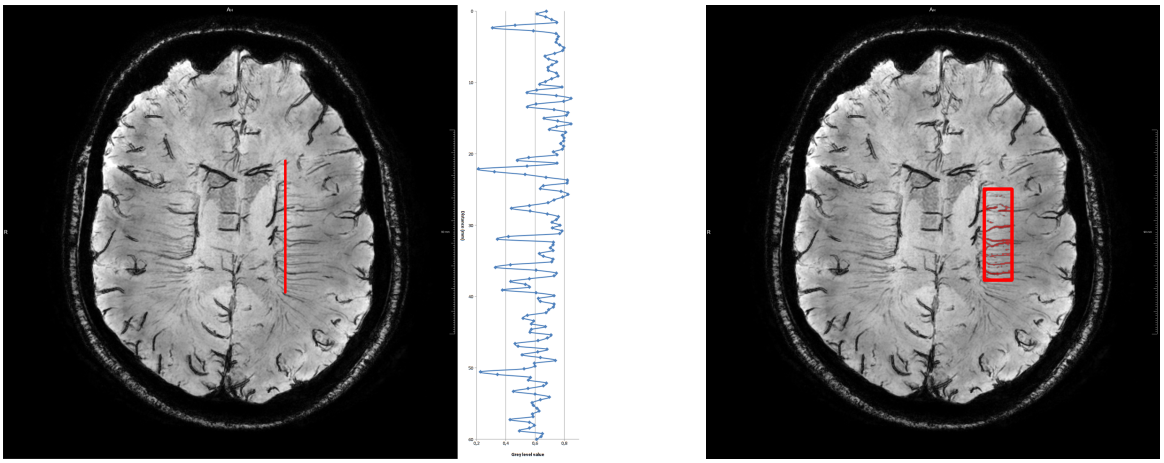

(a) Illustration of the method proposed by De Guio et al. A 6 cm long line-segment is automatically positioned in the semioval centre on a 6 mm thick minimum intensity projection slab. A profile curve of the intensities (graph on the right) along the line-segment is obtained. Vessels are counted based on local minima from the second derivative and local signal decrease criteria.[4]

(b) Illustration of the method proposed by Sinnecker et al. A region-of-interest of 1×4 cm is manually positioned on three contiguous slices. Veins are counted manually and the "periventricular venous area" is computed by thresholding (red voxels in this illustration).[3]

Figure 2: Illustrations of the methods proposed by De Guio et al. and Sinnecker et al.

Since periventricular veins can be visualized on 7.0 T MRI,[5] there is an interest in the automated detection and quantification of these veins. So far, De Guio et al.[4] and Sinnecker et al.[3] have proposed techniques to do this. De Guio et al. automatically position a line-segment through the semioval centre and inspect the intensity profile curve to extract periventricular veins that intersect the line-segment. This approach is illustrated in Figure 2a. Sinnecker et al. manually define a fixed region-of-interest of 1×4 cm on a slice tangential to the roof of the lateral ventricles. By thresholding on the intensities within this region-of-interest, venous voxels are selected. This approach is illustrated in Figure 2b.

Although both techniques have been applied successfully by their respective authors, there are several limitations. First and foremost, both consider only a small and limited section of the brain and do not capture the full 3D distribution of all periventricular veins.[6–8] Next, no quantitative evaluation of the results is given. Lastly, the work of Sinnecker et al. requires manual initialisation and is performed on images with a limited spatial resolution (slice thickness of 2 mm), possibly hampering reliable detection of periventricular veins that are often sub-millimetre in diameter.

In this proof of principle study, we will assess the feasibility of a new technique that automatically detects all periventricular veins in the brain. This technique consists of two steps. First, the definition of a proper region-of-interest that captures the full 3D distribution of periventricular veins. Secondly, the detection of periventricular veins in this region-of-interest using shape and intensity information. Optimal settings for all parameters of the proposed technique will be empirically determined. Finally, a human observer will inspect the images and the automatically detected veins.

2. METHODS AND MATERIALS

2.1 Participants

For this study, two healthy participants (1 male, 23 years; 1 female, 34 years) were included. Written informed consent was given by both participants.

2.2 MRI acquisition

MRI acquisition was performed on a 7.0 T MR system (Philips Healthcare, Cleveland, OH, USA), with a 32-channel receive head coil (Nova Medical, Wilmington, MA, USA) and a volume transmit. A 3D dual-echo gradient echo sequence was acquired (TR: 20 ms; first TE: 6.9 ms; second TE: 15.8 ms) and the images were reconstructed to $0.39 \times 0.39 \times 0.35$ mm^3. A 3D T1-weighted sequence was acquired (TR: 4.8 ms; TE: 2.2 ms; TI: 1240 ms; TR of inversion pulses: 3500 ms; flip angle: 8°) and reconstructed to $0.66 \times 0.66 \times 0.50$ mm^3.

2.3 Region-of-interest definition

Periventricular veins drain venous blood from the brain towards the caudate vein of Schlesinger. This vein is situated parallel to and in close proximity of the lateral ventricles. As an region-of-interest, we propose to use an expanded ventricular surface, because periventricular veins have to intersect with this surface to reach the vein of Schlesinger. This is shown in Figure 4. A CSF segmentation is obtained on the T1 scan with a unified segmentation approach as implemented in SPM12b.[9] The CSF atlas of the MNI152 template is aligned with the T1 scan using elastix,[10–12] allowing the extraction of the lateral ventricles from the segmentation. Next, the T1 scan is registered to the T2* image and the resulting transformation is applied to the ventricle segmentation. The ventricular surface is expanded by 5 mm, which is enough to extend past the caudate vein of Schlesinger. This is demonstrated in Figure 3. Caudally, the surface is restricted by a plane that touches the genu and splenium of the corpus callosum and is aligned with the Sylvian fissures. The interhemispheric fissure[13] and the surrounding cortex are removed from the surface as well, since no veins should occur there. All periventricular veins intersect with this surface, as can be appreciated in Figures 3 and 4.

2.4 Vein detection

Periventricular veins are visualised on the second echo of our T2* acquisition. The intensities of this scan are normalized to a range from 0 to 1, by histogram scaling between 0 and the 95th percentile of the intensities within the ventricle segmentation.

The well-known vesselness algorithm is computed on this image to identify all veins.[14,15] A hysteresis thresholding approach is applied on the vesselness image to detect veins and discard any false positives. All voxels on the inflated ventricular surface with a vesselness value above the low threshold T_{low} are considered potential candidates. Local maximum filtering is applied to suppress multiple detections of the same vein. Next, each candidate is used as the seed point of a bidirectional tubular tracking algorithm.[16] A few steps of the tubular tracking algorithm are computed on the original vesselness image. The candidate is considered to be a true periventricular vein if (1) the tubular tracking can track a vein originating from the candidate point and (2) within a few steps there is a vesselness value above the high threshold T_{high}.

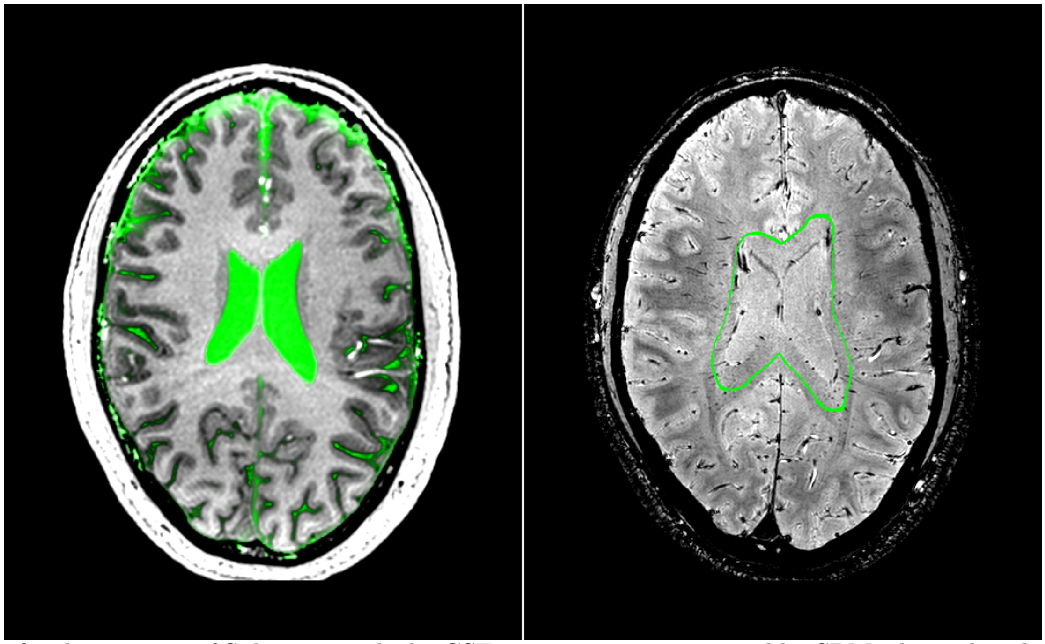

Figure 3: Left: the T1 scan of Subject 1 with the CSF segmentation generated by SPM12b overlayed in green. In this view, the T1 scan has been registered to the T2* scan (right). The ventricles were extracted and expanded by 5 mm, resulting in the green surface shown on the right.

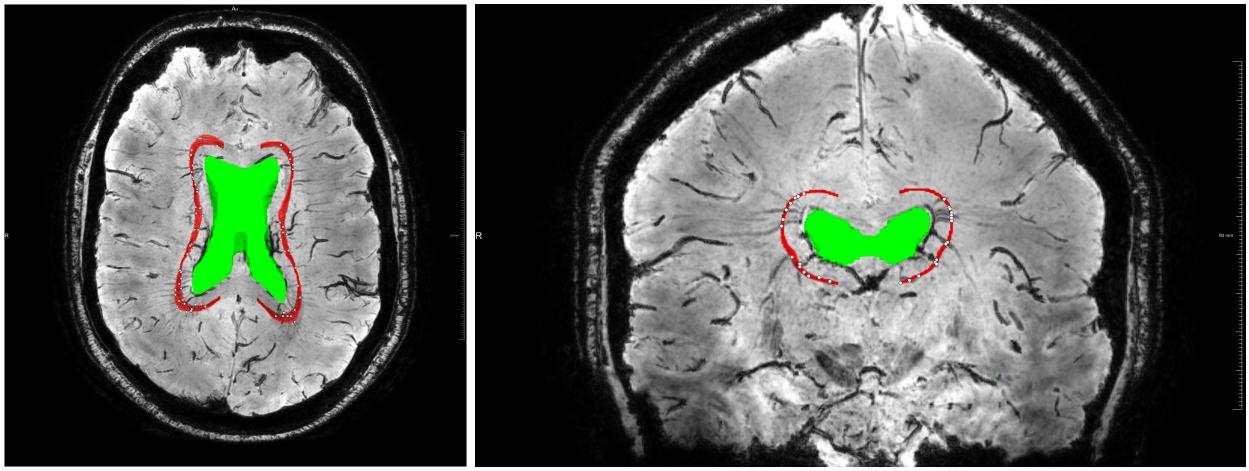

(a) (b)

Figure 4: an axial (a) and coronal (b) view of the second echo of a T2* scan. Both views are a minIP slab of 3.5 mm (= 10 slices). In green, the segmented ventricles. In red, the expanded surface, through which the periventricular veins cross. White dots are the automatically detected veins.

2.5 Experiments

Values of T_{high} and T_{low} will be set empirically, by visual inspection of the vesselness filter on a few slices in one of the two subjects.

Next, the proposed technique will be used to detect all periventricular veins in the scans of both subjects. All detected locations will be presented to a human observer for visual inspection. Any false positive detections will be censored and the positive predictive value will be computed.

Finally, a few randomly selected slices will be presented to a human observer, to identify any veins that were missed (false negatives). This will be used to compute the sensitivity of the proposed technique.

3. RESULTS

Inspection of the vesselness filter showed that most veins have a vesselness value above $T_{high} = 0.04$. Smaller veins with fluctuating intensities, owing to the partial volume effect, might not have that high of a vesselness value at the intersection with the expanded ventricular surface. Therefore, $T_{low} = 0.5 * T_{high} = 0.02$.

After applying the method, 441 locations were detected in Subject 1 and 439 locations were detected in Subject 2. Visual inspection of these locations showed that 87.6 % were true periventricular veins. Visual inspection of 4 random slabs, each slab containing 7 slices (2.45 mm), showed that the method achieved a sensitivity of 95.1 % (137 out of 144 veins detected).

4. DISCUSSION

To our knowledge, this is the first study to show a fully automated detection of all visible periventricular veins in the brain, with a high positive predictive value and an excellent sensitivity.

The expanded ventricular surface captures all periventricular veins that drain venous blood from the deep white matter towards the subependymal veins, such as the caudate vein of Schlesinger. This is a significant advantage over existing methods that use a 1D line-segment or a 2D rectangular region-of-interest. These limited regions-of-interest may miss many veins that are situated in the brain in their typical (3D) fan-pattern. Venous changes related to small vessel disease potentially occur throughout the brain and the proposed 3D region-of-interest captures all these locations. A small region around the interhemispheric fissure was removed, since that contains mostly CSF and the grey matter of the cortex. Periventricular veins that drain the white matter should not be present at these locations. Furtermore, the CSF in the sulci might cause false positive responses in the vesselness filter.

All individual periventricular veins intersected with our strategically positioned surface and are identified based on shape and intensity features. The well-known vesselness filter[14,15] is able to highlight the individual periventricular veins in the scans. However, this filter has a somewhat limited ability to enhance small veins that consist of partial volume effect voxels. Because of this, there can be a limited response of the vesselness filter at the intersection point of a periventricular vein and the expanded ventricular surface. To ensure that all veins are detected, we apply a double-thresholding approach with a lenient lower threshold T_{low} at the expanded ventricular surface. Each location that passes this threshold is used as a seedpoint to a tubular tracking algorithm. If a vein can be tracked successfully and has a vesselness response above T_{high}, this is considered a real vein.

Solely using threshold T_{high} would have resulted in many false negatives and consequently a low sensitivity. Only using T_{low} would have resulted in too many false positives and consequently a low positive predictive value. The double-thresholding approach proves to be a good trade-off between sensitivity and positive predictive value. If this technique would be implemented in a semi-automated workflow for the assessment of periventricular veins, a user can adapt T_{high} and T_{low} to his own needs, possibly preferring sensitivity over positive predictive value or vice versa. When a high sensitivity is required and even the tiniest veins need to be detected, T_{high} or T_{low} can be further reduced. This will probably reduce the positive predictive value and increase the time required to visually censor false positive detections. When time-constraints are tight or one is only interested in the larger veins, T_{high} or T_{low} could be increased.

The values for T_{high} and T_{low} are set empirically in this approach. To do so, the vesselness response at the location of periventricular veins intersecting the expanded ventricular surface was inspected at a few slices selected from Subject 2. This limited amount of training information proofed to be representative for the scans of both subjects. Owing to the high quality scans obtained from the 7.0 T MRI scanner, the visual appearance and properties of the periventricular veins is consistent throughout the semioval centre of both subjects. Acquiring high quality scans might be more challenging in the future, when this method will be applied in elderly subjects or patients, who demonstrate more head motion.[17]

In our future work, we will include more participants to evaluate the proposed method. Besides detecting and counting individual periventricular veins, more advanced quantification measures should be introduced. Individual veins can be inspected for length, lumen, tortuosity, or other properties. All detected veins combined can be used to investigate venous density at specific brain locations. Alterations to these veins might be indicative

for underlying pathological processes in the context of ageing, cognitive decline, or small vessel disease.[18,19] Quantification measures that can be used to assess subjects or compare groups of subjects will further advance research into these venous changes.

5. CONCLUSIONS

A new method for the automated detection of periventricular veins was presented in this proof-of-principle study and values for its two most important parameters T_{high} and T_{low} were determined. The results of the method are promising and show a high detection rate.

The expanded ventricular surface was able to capture all visible periventricular veins that drain towards the subependymal veins. This is an improvement over existing methods that use a 1D line-segment or a 2D rectangular region-of-interest. These limited regions-of-interest miss many veins that are situated in the brain in their typical (3D) fan-pattern. To our knowledge, this is the first work to present a quantitative evaluation of the detection method.

Future work will include more participants to evaluate the proposed method and comparisons between healthy and pathological brains.

6. ACKNOWLEDGMENTS

This study was financially supported by the project Brainbox (Quantitative analysis of MR brain images for cerebrovascular disease management), funded by the Netherlands Organisation for Health Research and Development (ZonMw) in the framework of the research programme IMDI (Innovative Medical Devices Initiative); project 104002002. This work was also supported by a Vidi grant from ZonMw, The Netherlands Organisation for Health Research and Development [91711384], to GJB. JZ received funding from the European Research Council under the European Unions Seventh Framework Programme (FP7/2007-2013) / ERC grant agreement №337333. We acknowledge the use of MeVisLab (MeVis Medical Solutions AG, Bremen, Germany[20]).

REFERENCES

[1] Pantoni, L., "Cerebral small vessel disease: from pathogenesis and clinical characteristics to therapeutic challenges," *The Lancet Neurology* **9**(7), 689 – 701 (2010).

[2] van Veluw, S. J., Zwanenburg, J. J., Hendrikse, J., van der Kolk, A., Luijten, P. R., and Biessels, G. J., [*Trends in Neurovascular Interventions*], vol. 119 of *Acta Neurochirurgica Supplement*, ch. High Resolution Imaging of Cerebral Small Vessel Disease with 7 T MRI, 125–130, Springer International Publishing (2014).

[3] Sinnecker, T., Bozin, I., Drr, J., Pfueller, C. F., Harms, L., Niendorf, T., Brandt, A. U., Paul, F., and Wuerfel, J., "Periventricular venous density in multiple sclerosis is inversely associated with t2 lesion count: a 7 tesla mri study," *Multiple Sclerosis Journal* **19**(3), 316–325 (2013).

[4] De Guio, F., Vignaud, A., Ropele, S., Duering, M., Duchesnay, E., Chabriat, H., and Jouvent, E., "Loss of venous integrity in cerebral small vessel disease: A 7-t mri study in cerebral autosomal-dominant arteriopathy with subcortical infarcts and leukoencephalopathy (cadasil)," *Stroke* **45**(7), 2124–2126 (2014).

[5] Zwanenburg, J. J., Versluis, M. J., Luijten, P. R., and Petridou, N., "Fast high resolution whole brain t2* weighted imaging using echo planar imaging at 7 t," *NeuroImage* **56**(4), 1902 – 1907 (2011).

[6] Schlesinger, B., "The venous drainage of the brain, with special reference to the galenic system," *Brain* **62**(3), 274–291 (1939).

[7] Hooshmand, I., Rosenbaum, A. E., and Stein, R. L., "Radiographic anatomy of normal cerebral deep medullary veins: criteria for distinguishing them from their abnormal counterparts," *Neuroradiology* **7**(2), 75–84 (1974).

[8] Friedman, D. P., "Abnormalities of the deep medullary white matter veins: Mr imaging findings," *AJR. American journal of roentgenology* **168**(4), 1103–1108 (1997).

[9] Ashburner, J. and Friston, K. J., "Unified segmentation," *NeuroImage* **26**, 839–851 (2005).

[10] Fonov, V. S., Evans, A. C., Botteron, K., Almli, C. R., McKinstry, R. C., and Collins, D. L., "Unbiased average age-appropriate atlases for pediatric studies," *NeuroImage* **54**(1), 313 – 327 (2011).

[11] Klein, S., Staring, M., Murphy, K., Viergever, M. A., and Pluim, J. P. W., "elastix: A toolbox for intensity-based medical image registration," *IEEE Transactions on Medical Imaging* **29**, 196 –205 (jan. 2010).

[12] Fonov, V. S., Evans, A. C., McKinstry, R. C., Almli, C. R., and Collins, D. L., "Unbiased nonlinear average age-appropriate brain templates from birth to adulthood," *NeuroImage* **47, Supplement 1**, S102 (2009). Organization for Human Brain Mapping 2009 Annual Meeting.

[13] Kuijf, H. J., Leemans, A., Viergever, M. A., and Vincken, K. L., "Assessment of methods to extract the mid-sagittal plane from brain mr images," in [*Proc. SPIE*], **8673**, 86731K (2013).

[14] Frangi, A., Niessen, W., Vincken, K., and Viergever, M., "Multiscale vessel enhancement filtering," in [*Medical Image Computing and Computer-Assisted Intervention MICCAI98*], Wells, W., Colchester, A., and Delp, S., eds., *Lecture Notes in Computer Science* **1496**, 130–137, Springer Berlin Heidelberg (1998).

[15] Sato, Y., Nakajima, S., Shiraga, N., Atsumi, H., Yoshida, S., Koller, T., Gerig, G., and Kikinis, R., "Three-dimensional multi-scale line filter for segmentation and visualization of curvilinear structures in medical images," *Medical Image Analysis* **2**(2), 143–168 (1998).

[16] Friman, O., Hindennach, M., Khnel, C., and Peitgen, H.-O., "Multiple hypothesis template tracking of small 3d vessel structures," *Medical Image Analysis* **14**(2), 160–171 (2010).

[17] Zeng, L. L., Wang, D., Fox, M. D., Sabuncu, M., Hu, D., Ge, M., Buckner, R., and Liu, H., "Neurobiological basis of head motion in brain imaging," *Proceedings of the National Academy of Sciences* **111**(16), 6058–6062 (2014).

[18] Moody, D. M., Brown, W. R., Challa, V. R., Ghazi-Birry, H. S., and Reboussin, D. M., "Cerebral microvascular alterations in aging, leukoaraiosis, and alzheimer's diseasea," *Annals of the New York Academy of Sciences* **826**(1), 103–116 (1997).

[19] Moody, D. M., Thore, C. R., Anstrom, J. A., Challa, V. R., Langefeld, C. D., and Brown, W. R., "Quantification of afferent vessels shows reduced brain vascular density in subjects with leukoaraiosis," *Radiology* **233**(3), 883–890 (2004).

[20] Ritter, F., Boskamp, T., Homeyer, A., Laue, H., Schwier, M., Link, F., and Peitgen, H.-O., "Medical image analysis: A visual approach," *IEEE Pulse* **2**, 60–70 (Nov.-Dec. 2011).